Acoustic and Biomedical Engineering 2014

Sound Energy Field in a System of Coupled Rooms

M. Meissner
Institute of Fundamental Technological Research of the Polish Academy of Sciences
A. Pawińskiego 5B, 02–106 Warsaw, Poland

The paper presents a theoretical basis of calculations of the sound intensity in enclosed spaces and shows results of numerical visualization of the active intensity in a room with absorptive walls formed by two coupled rectangular subrooms. The study was focused on the low-frequency range, therefore to describe the active and reactive intensities, the modal theory of room acoustics was applied. Space distribution of eigenfunctions, modal frequencies and modal damping coefficients were calculated numerically using the forced oscillator method (FOM) and the finite difference time-domain (FDTD) method. Based on theoretical and numerical results, the computer program has been developed to simulate the active intensity vector field when the room is excited by a harmonic point source. Calculation data have shown that the active intensity was extremely sensitive to position of the source since at a fixed source frequency, different source locations always generate different distributions of characteristic objects of the active sound field such as energy vortices and stagnation points. Because of complex room shape, the vortex centers are in most cases positioned irregularly inside the room. Almost regular arrangement of vortices was found only in the case when the source frequency was tuned to the frequencies of modes which were strongly localized in one of the subrooms.

DOI: 10.12693/APhysPolA.125.A-103
PACS: 43.55.Br, 43.55.Ka, 43.20.Ks

1. Introduction

The sound intensity has gained much attention in the past because this quantity is very useful for analyzing the energy properties of a sound field in both open and enclosed spaces. The concept of the sound field energy streamlines has been introduced into acoustics for the first time by Waterhouse et al. [1]. Local properties of energy streamlines at singular points of two- and three-dimensional sound fields, such as vortices and stagnation points, have been examined by Chien and Waterhouse [2] and Zhe [3]. The concept of complex sound intensity has been developed by Mann et al. [4] and treated in Fahy's book [5]. New instantaneous intensimetric quantities in general stationary fields called the radiating and oscillating intensities have been presented and measured by Stanzial and Prodi [6].

The energy-related quantities of a sound field in enclosed spaces have been also studied, although for a long time the main interest of room acoustics was directed to the analysis of sound pressure field in enclosures. In [7], Waterhouse has demonstrated existence of energy vortices in rooms on theoretical grounds. The connection between the mean energy velocity, the reverberation time and the angular momentum density has been studied by Stanzial and Schiffrer [8]. Statistical properties of the sound intensity in reverberant rooms subjected to pure-tone excitation have been examined by Jacobsen and Molares [9]. In recent papers of the present author [10–12], space distributions of energy density and sound intensity in a steady-state acoustic field inside coupled rooms and irregular enclosures were analyzed using the modal expansion method supported by computer implementations. In turn, the special acoustic properties of coupled-room systems such as the mode degeneration due to modification of the coupling area, confinement of an acoustic energy in a part of room system called the localization of modes, and a considerable difference between a rate of sound decay in early and late stages of the reverberant process, known as a double sloped decay were investigated by the present author in [13] and [14].

This paper is organized as follows. Section 1 contains a brief review of the papers devoted to energy properties of a sound field in both open and enclosed spaces. Section 2, in turn, shows a theoretical basis of sound intensity calculations in enclosures with absorptive walls. This section summarizes theoretical findings of the author formerly presented in [11]. Subsection 3.1 reveals details about geometry of coupled room system under consideration. Subsection 3.2 shortly outlines the numerical method and provides an analysis of visualized distributions of the active sound intensity. Calculations are aimed at examination of the impact of sound source parameters on a structure of the active intensity field and locations of vortices and stagnation points. Finally, Section 4 summarizes and concludes the paper.

2. Theoretical basis of sound intensity calculations

In order to calculate distribution of the sound intensity vector field in enclosures, knowledge of distributions of the sound pressure and the acoustic particle velocity is needed. Traditionally, in the low-frequency range, the classical modal analysis is used to describe acoustic quantities in a room with walls covered with materials characterized by low sound absorption. When the room is excited by a pure-tone point source, the sound pressure in steady-state can be expanded in terms of rigid-walled modes determined by eigenfunctions φ_m and the modal

angular frequencies ω_m, and the associated damping coefficient r_m for each of these modes [11]

$$p(\boldsymbol{r},t)=\sum_{m=0}^{\infty}(\alpha_m+\mathrm{i}\beta_m)\varphi_m(\boldsymbol{r})\varphi_m(\boldsymbol{r}_0)e^{\mathrm{i}\omega t}, \tag{1}$$

where the modal factors α_m and β_m given by

$$\alpha_m=\frac{\sqrt{8\pi\rho c\mathcal{P}_0}(\omega^2-\omega_m^2)c^2}{(\omega^2-\omega_m^2)^2+4r_m^2\omega^2}, \tag{2}$$

$$\beta_m=\frac{2\sqrt{8\pi\rho c\mathcal{P}_0}\omega r_m c^2}{(\omega^2-\omega_m^2)^2+4r_m^2\omega^2} \tag{3}$$

are the real and imaginary parts of the amplitude term, ω is the source angular frequency, c is the sound speed, ρ is the air density, $\mathcal{P}_0$ is the source power, while $\boldsymbol{r}=(x,y,z)$ and $\boldsymbol{r}_0=(x_0,y_0,z_0)$ determine the observation and the source point, respectively. The modal damping coefficient is given by

$$r_m=\frac{\rho c^2}{2}\int_S\frac{\varphi_m^2(\boldsymbol{r})}{Z}\,\mathrm{d}s, \tag{4}$$

where Z is the wall impedance and S is the surface area of room walls. Equation (1) shows that in steady-state, distribution of the sound pressure is as follows

$$p(\boldsymbol{r},t)=P(\boldsymbol{r})e^{\mathrm{i}[\varphi(\boldsymbol{r})+\omega t]}, \tag{5}$$

where P is the pressure amplitude and φ is the spatial dependent phase function. Further, by applying the Euler's equation of motion, the corresponding particle velocity $\boldsymbol{u}$ can be calculated as

$$\boldsymbol{u}(\boldsymbol{r},t)=\frac{1}{\rho\omega}\left[-P(\boldsymbol{r})\nabla\varphi(\boldsymbol{r})+\mathrm{i}\nabla P(\boldsymbol{r})\right]e^{\mathrm{i}[\varphi(\boldsymbol{r})+\omega t]}=\frac{1}{\rho\omega}\sum_{m=0}^{\infty}(-\beta_m+\mathrm{i}\alpha_m)\varphi_m(\boldsymbol{r}_0)\nabla\varphi_m(\boldsymbol{r})e^{\mathrm{i}\omega t}. \tag{6}$$

In terms of these quantities, the complex sound intensity vector $\boldsymbol{I}_c$ is expressed as

$$\boldsymbol{I}_c=\frac{1}{2}p\boldsymbol{u}^*=\boldsymbol{I}+\mathrm{i}\boldsymbol{Q}, \tag{7}$$

where the asterisk in the superscript denotes the complex conjugate and $\boldsymbol{I}$ and $\boldsymbol{Q}$ are the active and the reactive sound intensity, respectively. Substituting Eqs. (1), (5) and (6) into Eq. (7) yields the following expressions for sound intensity components

$$\boldsymbol{I}=-\frac{P^2(\boldsymbol{r})\nabla\varphi(\boldsymbol{r})}{2\rho\omega}=\frac{1}{2\rho\omega}\sum_{m=0}^{\infty}\sum_{n=0}^{\infty}(\alpha_n\beta_m-\alpha_m\beta_n)\times\varphi_m(\boldsymbol{r}_0)\varphi_n(\boldsymbol{r}_0)\varphi_m(\boldsymbol{r})\nabla\varphi_n(\boldsymbol{r}), \tag{8}$$

$$\boldsymbol{Q}=-\frac{P(\boldsymbol{r})\nabla P(\boldsymbol{r})}{2\rho\omega}=-\frac{c^2}{\omega}\nabla w_p=-\frac{1}{2\rho\omega}\sum_{m=0}^{\infty}\sum_{n=0}^{\infty}(\alpha_m\alpha_n+\beta_m\beta_n)\times\varphi_m(\boldsymbol{r}_0)\varphi_n(\boldsymbol{r}_0)\varphi_m(\boldsymbol{r})\nabla\varphi_n(\boldsymbol{r}), \tag{9}$$

where $w_p=P^2/4\rho c^2$ is the potential energy density. Equation (9) confirms that the reactive intensity vector $\boldsymbol{Q}$ is always irrotational. On the contrary, the active intensity $\boldsymbol{I}$ represents a rotational vector field because the curl of right-hand side of Eq. (8) is non-zero and equals

$$\nabla\times\boldsymbol{I}=\frac{1}{\rho\omega}P(\boldsymbol{r})\nabla\varphi(\boldsymbol{r})\times\nabla P(\boldsymbol{r})=\frac{\omega}{c^2}\frac{\boldsymbol{I}\times\boldsymbol{Q}}{w_p}=\frac{1}{2\rho\omega}\sum_{m=0}^{\infty}\sum_{n=0}^{\infty}(\alpha_n\beta_m-\alpha_m\beta_n)\varphi_m(\boldsymbol{r}_0)\varphi_n(\boldsymbol{r}_0)\times\nabla\varphi_m(\boldsymbol{r})\times\nabla\varphi_n(\boldsymbol{r}), \tag{10}$$

thus, when a room is excited by a harmonic sound source, there is a circulating energy flow in a steady-state sound field.

3. Results of computer simulation

The main objective of computer simulation presented in the following was to examine a flow of acoustic energy in harmonic, steady-state sound field generated by a point source in a system of coupled rooms. In other words, the simulation was aimed at visualization of direction and magnitude of the active intensity and determination of the curl of this vector in order to identify the rotating energy flow in the sound field. These vector quantities can be calculated from Eqs. (8) and (9) for the known source and room parameters such as the source frequency, position, and power, and for natural frequencies and mode shapes. When shape of a room becomes complicated, the modal characteristics of the room are determined by the use of numerical methods.

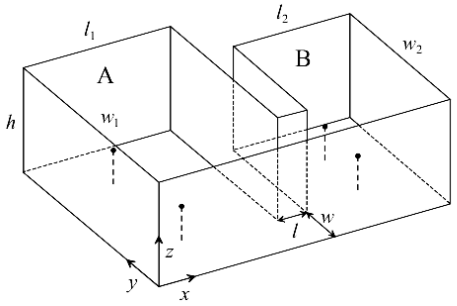

Fig. 1. The analyzed room system containing two coupled subrooms A and B. Points indicate positions of a source, whereas dashed lines denote distance between the source and the floor.

3.1. Room system description

The computer simulation was carried out for the room system shown schematically in Fig. 1. The enclosure consists of two rectangular subrooms having the same height. The subrooms are connected to each other via an opening, so that the acoustic energy can be transmitted between them. The subrooms dimensions assumed in the numerical model are the following: $l_1=5$ m, $l_2=4$ m, $w_1=8$ m, $w_2=6$ m and $h=3$ m. The opening between subrooms has the height h, the width w of 1.6 m and the thickness l of 1 m. It was assumed that the absorbing material was uniformly distributed on the subrooms' walls and the room system was slightly damped, i.e., the wall impedance was such that $|Z|/\rho c\gg 1$ and $\mathrm{Re}(Z)\gg\mathrm{Im}(Z)$.

3.2. Numerical method

The first step towards determining the active intensity $\boldsymbol{I}$ consisted in computation of eigenfunctions φ_m and modal frequencies ω_m. Since the analyzed room is irregularly shaped, the functions φ_m were calculated numerically using the forced oscillator method (FOM) and the finite difference time-domain (FDTD) method. The FOM is based on the rule that the response of linear system to a harmonic excitation is large when the driving frequency is close to the modal frequency. In this method the eigenvalue problem for enclosure with rigid walls is solved by making use of analytical solution of the inhomogeneous wave equation

$$\nabla^2 f(\boldsymbol{r},t) - \frac{1}{c^2}\frac{\partial^2 f(\boldsymbol{r},t)}{\partial t^2} = q(\boldsymbol{r})\cos(\omega t), \tag{11}$$

which satisfies the Neumann boundary condition and homogeneous initial conditions

$$f(\boldsymbol{r},t)_{t=0} = [\partial f(\boldsymbol{r},t)/\partial t]_{t=0} = 0. \tag{12}$$

It can be easily found that solution to this problem has the form

$$f(\boldsymbol{r},t) = c^2 \sum_{m=0}^{\infty} \varphi_m(\boldsymbol{r}) \int_V q(\boldsymbol{r})\varphi_m(\boldsymbol{r})\,\mathrm{d}v \times \frac{\cos(\omega t) - \cos(\omega_m t)}{\omega^2 - \omega_m^2}, \tag{13}$$

where V is the room volume. When the driving frequency ω is close to the modal frequency ω_m, then for sufficiently large time τ only the term connected with the mode number m contributes the sum in Eq. (13), so one can write $f(\boldsymbol{r},\tau) \approx a\varphi_m(\boldsymbol{r})$, where a is a constant. The eigenfunction φ_m is determined after a normalization procedure which results in elimination of the constant. Finally, the use of formula

$$\omega_m = c\left[-\int_V \varphi_m(\boldsymbol{r})\nabla^2\varphi_m(\boldsymbol{r})\,\mathrm{d}v\right]^{1/2}, \tag{14}$$

derived directly from the eigenvalue equation $\nabla^2\varphi_m + (\omega_m/c)^2\varphi_m = 0$, enables to calculate ω_m. In the FDTD algorithm, uniform grids with spacing $\Delta s = 0.1$ m were used and in order to ensure a stability of a numerical scheme, the time step Δt was set to 10^{-4} s yielding the Courant number $C_r = c\Delta t/\Delta s$ of 0.343.

By means of the numerical method described above 150 modes with frequencies $f_m = \omega_m/2\pi$ ranging from 0 Hz to 170 Hz were found. Subsequently, when mode shapes were known the damping coefficients r_m were calculated from Eq. (4) assuming that $|Z|/\rho c = 100$. The modal factors α_m and β_m were determined for the source power $\mathcal{P}_0$ of 10^{-3} W.

3.3. Distributions of active sound intensity

Graphs in Fig. 2 show example vector fields $\boldsymbol{I}$ obtained on the observation plane situated at a constant height from the floor. They illustrate changes in the active intensity distributions when the point sound source with a constant frequency is located at different positions in the room space. As can be seen, distributions of active intensity streamlines on the observation plane are very complex and characteristic objects in the vector field $\boldsymbol{I}$ are irregularly located vortices. This type of vortices form such patterns of flow where sound energy gyrates around closed paths. Note that vortices of the active intensity are particulary visible in the subroom where the source is located and this proves that the circulating flow of sound energy, which is evident in the steady-state, is highly influenced by the source position.

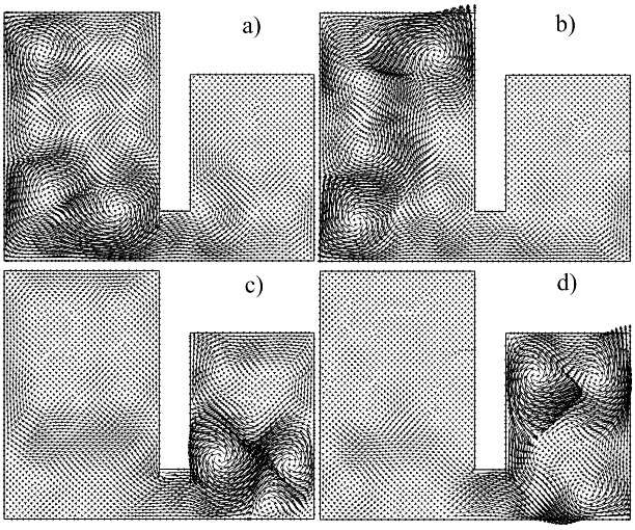

Fig. 2. Distribution of the active sound intensity $\boldsymbol{I}$ on the observation plane $z = 1.5$ m for different source positions (x_0, y_0, z_0) (in meters): (a) (2,2,1); (b) (2,6,1); (c) (8,2,1); (d) (8,4,1). The source frequency is set to 75 Hz.

Another singular point of the intensity $\boldsymbol{I}$ field is the stagnation point which represents the point where there is separation of the vortex region from the region where the intensity vectors form open lines. The pressure is zero at vortex centers, while at stagnation points the real component of the particle velocity vanishes. Thus, according to Eqs. (6), (8) and (9), the active intensity $\boldsymbol{I}$ is zero, both at vortex centers and stagnation points, whereas the reactive intensity $\boldsymbol{Q}$ is zero at vortex centers. The first property is clearly visible in Fig. 3 where distributions of the magnitude $|\boldsymbol{I}|$ for considered source positions are shown. The plots have a form of filled contour maps, where black and white colors denote zero and maximum values of $|\boldsymbol{I}|$, respectively. In order to better differentiate between vortex and stagnation points, in Fig. 4 their positions are indicated by easily distinguishable symbols. They are intentionally located on mapped distributions of $|\nabla \times \boldsymbol{I}|$ to show what is the circulation of the active intensity at vortex centers because by virtue of Eq. (10), at stagnation points the quantity $\nabla \times \boldsymbol{I}$ is always equal to zero. The graphs in Fig. 4 highlights the fact that at a vortex center the magnitude of circulation of $\boldsymbol{I}$ reaches a value very close to a local maximum although the pres-

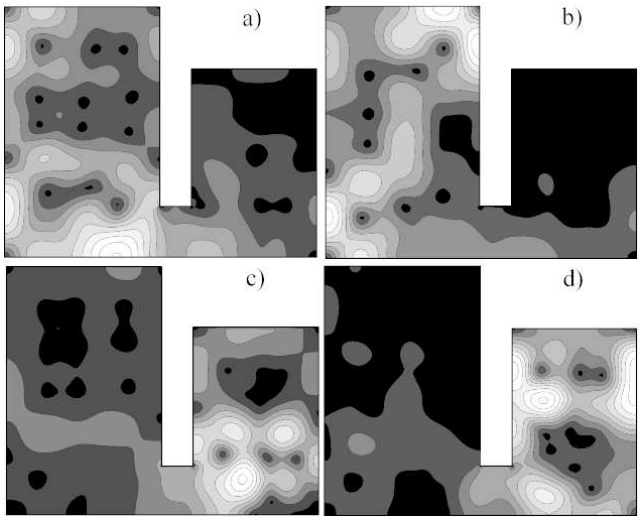

Fig. 3. Distribution of $|\boldsymbol{I}|$ on the observation plane z = 1.5 m for different source positions (x_0, y_0, z_0) (in meters): (a) (2,2,1); (b) (2,6,1); (c) (8,2,1); (d) (8,4,1). The source frequency is set to 75 Hz. Black and white colors denote zero and maximum values of $|\boldsymbol{I}|$, respectively.

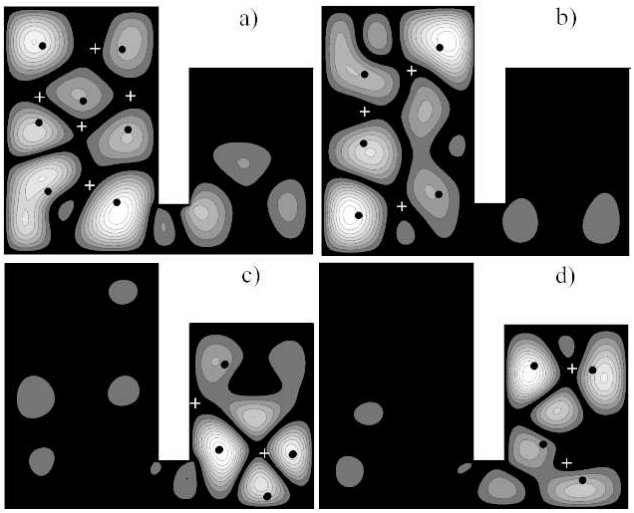

Fig. 4. Distribution of $|\nabla \times \boldsymbol{I}|$ on the observation plane z = 1.5 m for different source positions (x_0, y_0, z_0) (in meters): (a) (2,2,1); (b) (2,6,1); (c) (8,2,1); d) (8,4,1). The source frequency is set to 75 Hz. Black and white colors denote zero and maximum values of $|\nabla \times \boldsymbol{I}|$, respectively. Black points indicate centers of vortices, whereas white crosses represent positions of stagnation points.

sure vanishes in this point. According to Eqs. (6) and (10), the curl of $\boldsymbol{I}$ is proportional to the vector product of real and imaginary parts of velocity amplitude

$$\nabla \times \boldsymbol{I} = -\rho\omega[\boldsymbol{U}_r \times \boldsymbol{U}_i], \tag{15}$$

where $\boldsymbol{U}_r = -P\nabla\varphi/\rho\omega$ and $\boldsymbol{U}_i = \nabla P/\rho\omega$. Since at the vortex center there cannot be an infinite amount of energy, $\boldsymbol{U}_r$ is finite at this point. On the other hand, the

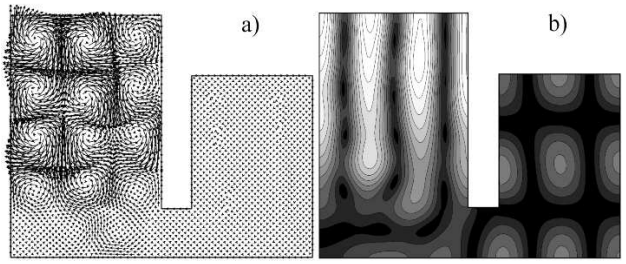

Fig. 5. Distributions of (a) the active sound intensity $\boldsymbol{I}$ and (b) the pressure amplitude P on the observation plane z = 1.5 m for the source frequency of 103.4 Hz and the source position: x_0 = 2 m, y_0 = 3 m, z_0 = 1 m. Black and white colors denote zero and maximum values of P, respectively.

pressure amplitude P should be zero at the vortex center, thus the magnitude $|\nabla\varphi|$ tends to infinity at this point. This means that the pressure phase φ is discontinuous at the vortex center.

The simulation results in Figs. 2–4 demonstrate that excitation of irregular enclosure by a harmonic sound source is associated with a formation of energy vortices which are irregularly located inside the room space. However, there are specific source frequencies for which the active intensity $\boldsymbol{I}$ vector field is characterized by almost regular distribution of vortices. This is the case when the source frequency is tuned to the natural frequency of modes which are localized in one of the subrooms. The example of such a situation is shown in Fig. 5a where a distribution of the active intensity $\boldsymbol{I}$ for the source frequency of 103.4 Hz is visualized. This frequency corresponds to the natural frequency of 43rd eigenmode which is strongly localized in the subroom A. In this case the modal localization also results in excitation of an intense standing wave that is clearly visible in the distribution of the sound pressure amplitude (Fig. 5b).

4. Conclusions

The paper reports numerical investigation into the prediction of energetic properties of a steady-state sound field generated inside two coupled subrooms by a harmonic sound source. Visualized distributions of energetic sound field have shown that characteristic objects in the active intensity vector field are energy vortices and stagnation points and positions of these objects are very sensitive to the location of a sound source. Calculations revealed also that, according to the theory, the active intensity should be zero, both at the vortex centers and stagnation points, whereas the reactive intensity should be zero at stagnation points. It was found that the magnitude of curl of the active intensity reaches a value very close to a local maximum at the vortex center. Vortices and stagnation points are usually located irregularly inside the room because of a complex room geometry. However, the almost regular arrangement of vortices can be

obtained when the source frequency is tuned to the natural frequency of mode which is strongly localized in one of the subrooms.

References

[1] R. Waterhause, T. Yates, D. Feit, Y. Liu, *J. Acoust. Soc. Am.* **78**, 758 (1985).

[2] C. Chien, R. Waterhouse, *J. Acoust. Soc. Am.* **101**, 705 (1997).

[3] J. Zhe, *J. Acoust. Soc. Am.* **107**, 725 (2000).

[4] J. Mann, J. Tichy, A. Romano, *J. Acoust. Soc. Am.* **82**, 17 (1987).

[5] F. Fahy, *Sound Intensity*, 2nd ed., E&FN Spon, London 1995.

[6] D. Stanzial, N. Prodi, *J. Acoust. Soc. Am.* **102**, 2033 (1997).

[7] R. Waterhouse, *J. Acoust. Soc. Am.* **82**, 1782 (1987).

[8] D. Stanzial, G. Schiffrer, *J. Sound Vib.* **329**, 931 (2010).

[9] F. Jacobsen, A. Molares, *J. Acoust. Soc. Am.* **129**, 211 (2011).

[10] M. Meissner, *Arch. Acoust.* **36**, 761 (2011).

[11] M. Meissner, *J. Acoust. Soc. Am.* **132**, 228 (2012).

[12] M. Meissner, *Appl. Acoust.* **74**, 661 (2013).

[13] M. Meissner, *Acta Phys. Pol. A* **118**, 123 (2010).

[14] M. Meissner, *Acta Phys. Pol. A* **119**, 1031 (2011).